PNAS
www.pnas.org

Supporting Information for

Arid1a is essential for intestinal stem cells through Sox9 regulation

Yukiko Hiramatsu, Akihisa Fukuda, Satoshi Ogawa, Norihiro Goto, Kozo Ikuta, Motoyuki Tsuda, Yoshihide Matsumoto, Yoshito Kimura, Takuto Yoshioka, Yutaka Takada, Takahisa Maruno, Yuta Hanyu, Tatsuaki Tsuruyama, Zhong Wang, Haruhiko Akiyama, Shigeo Takaishi, Hiroyuki Miyoshi, Makoto Mark Taketo, Tsutomu Chiba and Hiroshi Seno

Correspondence: Akihisa Fukuda MD, PhD
Email: fukuda26@kuhp.kyoto-u.ac.jp

This PDF file includes:

www.pnas.org/cgi/doi/10.1073/pnas.1804858116

Materials and Methods

Histologic analyses and immunostaining

For histologic analyses, mouse organs were isolated and fixed overnight in 4% paraformaldehyde, embedded in paraffin, and sectioned at a thickness of 5 μm. Sections were then deparaffinized, rehydrated, and stained with hematoxylin and eosin (H&E) or alcian blue, and counterstained with nuclear fast red (KPL). For immunohistochemical analyses, sections were incubated overnight at 4°C with primary antibody and washed with PBS. Washed sections were incubated with biotinylated secondary antibody for 1 hour at room temperature. Sections were then incubated with avidin biotin-peroxidase complex (Vector Laboratories), labeled with peroxidase, and coloured with diaminobenzidine substrate (Dako). For immunofluorescence, sections were incubated overnight at 4°C with primary antibody and washed with PBS. Washed sections were incubated with fluorescence conjugated secondary antibody (Invitrogen) for 1 hour at room temperature. Primary antibodies used in this study were obtained from the indicated suppliers: rabbit anti-Arid1a (1:500; ab182560, Abcam), mouse anti-Arid1b (1:200; ab57461, Abcam), rabbit anti-lysozyme (1:200; ab108508, Abcam), rabbit anti-Mmp7 (1:100; 3801S, Cell Signaling Technology), rabbit anti-chromogranin A (1:100; ab15160, Abcam), rabbit anti-Dclk1 (1:200; ab31704, Abcam), rat anti-Ki67 (1:100; 652402, BioLegend), rabbit anti-cleaved caspase 3 (1:200; 9664S, Cell Signaling Technology), mouse anti-E-cadherin (1:100; 610182, BD Transduction Laboratories), chicken anti-GFP (1:200; ab13970, Abcam), rat anti-Musashi-1 (1:1000; a gift from Dr. Okano, Keio University, School of Medicine, Department of Physiology, Tokyo, Japan), rabbit anti-Sox9 (1:10000; AB5535, Millipore), rabbit anti-Villin-1 (1:100; 2369S, Cell Signaling Technology), and rabbit anti-Hes1 (1:10000, gift from Dr. Sudo). Antigen retrieval for all primary antibodies was achieved by boiling in 10 mM citrate buffer pH 6.0 for 15 min. For quantitative analysis, cell counting or measurement was performed in at least ten sections from three animals for each genotype.

Electron microscopy

Electron microscopic analysis was performed using the standard method for mice. The mouse small intestine was placed in 4% paraformaldehyde with 2% glutaraldehyde for a minimum of 12 hours, and cut into 1 mm thick coronal sections. Next, sections were post-fixed in 1.0% osmium tetraoxide in 100 mM phosphate buffer, pH 7.4, for 2 hours at room temperature, and dehydrated in a series of graded ethanol solutions. After immersion in propylene oxide, samples were immersed in a mixture (1:1) of propylene oxide and Epon812 (LUVEAC-812, Nacalai Tesque, Japan) for 1.5 hours. Samples were then immersed in a mixture (1:3) of propylene oxide and Epon812 for 1.5 hours and finally immersed in only Epon812 for 12 hours. After immersion, samples were embedded in Epon812 resin according to the inverted beam capsule procedure and polymerized at 60°C for 3 days. The tissue samples were cut into ultrathin sections (70 nm) on an EM UC6 ultramicrotome (Leica, Germany). The ultrathin sections were examined with an H7650 electron microscope (Hitachi, Japan).

Crypt isolation

Crypts were isolated according to the protocol described previously(1-4). First, intestines were flushed with phosphate-buffered saline (PBS) and incised longitudinally after which villi were removed mechanically by scraping. Sections (0.5 mm) were incubated in EDTA (5 mM)/PBS for 30 min at 4°C per fraction of epithelium. After incubation, the epithelium was separated by vigorous shaking and the remaining intestinal tissue was placed in a new tube for collection of subsequent fractions. After isolation, crypt cells were pelleted, and passed through a 100 μm cell strainer.

qRT-PCR

Total RNA was extracted from tissues or isolated crypts using the RNeasy Micro Kit (Qiagen). Single-strand cDNA was synthesized using a Transcriptor First Strand cDNA Synthesis Kit (Roche Applied Science). Q-PCR was performed using SYBR Green I Master (Roche Applied Science) and LightCycler 480 (Roche Applied Science). Values were expressed as arbitrary units relative to GAPDH. Primers are listed in *SI Appendix*, Table S2.

Microarray analysis

Total RNA from isolated crypts of *Arid1a*$^{f/f}$ and *Villin-Cre; Arid1a*$^{f/f}$ mice intestines was examined using the SurePrint G3 Mouse GE v2 8x60K Microarray (Agilent). The raw data were quantified by Agilent Feature Extraction software (Agilent Technologies). Quantified data were normalized by the Gene Spring 14.5 software (Agilent Technologies). Unnamed genes were excluded. Differential expression analysis was performed using edgeR. As previously described, gene expression data were analyzed using the GSEA software and the Molecular Signature Database (MSigDB) provided by the Broad Institute of MIT and Harvard(5). The complete microarray data set is available from GEO (GSE110181).

β -Galactosidase (LacZ) staining

Freshly isolated small intestines were incubated in ice-cold fixative solution (PBS containing 4% paraformaldehyde, 5 mmol/L EGTA, 2 mmol/LMgCl2, 0.2% glutaraldehyde, and 0.02% NP-40) for 1 hour at 4°C. After washing twice in PBS for 20 minutes, tissues were incubated overnight at room temperature with LacZ substrate (PBS containing 5 mmol/L K3Fe(CN)6, 5 mmol/L K4Fe(CN)6, 2 mmol/L MgCl2, 0.02% NP-40, 0.1% sodium deoxycholate, and 1 mg/mL X-galactosidase). After washing twice in PBS for 20 minutes, tissues were fixed overnight at 4°C in 4% paraformaldehyde in PBS. Paraformaldehyde was removed, and the stained tissues were transferred to tissue cassettes.

Spheroid culture

Conditioned medium of L-cell line secreting Wnt3a, R-spondin3, and Noggin (L-WRN CM) was prepared as described previously(6). L-WRN was purchased from ATCC (ATCC; CRL3276). Isolated crypts of the proximal small intestine were embedded in Matrigel (BD Biosciences). For spheroid culture of normal epithelium, 50% L-WRN CM supplemented with 5 µmol/L Y-27632 (Tocris Bioscience) was added to each well. No passages were performed.

ChIP-qPCR and ChIP-Seq

SimpleChIP Plus Enzymatic Chromatin IP Kit (Magnetic Beads) (#9005, Cell Signaling Technology) was used for ChIP assay. Primers were designed as described previously and listed *SI Appendix*, Table S2. Negative control antibody (IgG) was included in the SimpleChIP Plus Enzymatic Chromatin IP Kit. Rabbit anti-Arid1a antibody (1:100; #12354, Cell Signaling Technology) was used in this study. Sequencing libraries were prepared using the TruSeq ChIP Sample Prep Kit (Illumina) following the manufacturer's instructions. The libraries were sequenced on the HiSeq 2500 sequencing platform using HiSeq SBS Kit v4 reagents with 2 x 101 cycles. ChIP-Seq reads were mapped to the mouse reference genome (mm10) by Bowtie (version 1.1.1). Enriched-regions (peaks) were determined using MACS2 peak caller (version 2.9.10) with a q-value cutoff of 0.05. Peaks were annotated by in-house scripts. MEME software (version 1.10.1) was used to identify the binding motif. GO analysis of all gene targets identified by peak calling analysis was performed as follows: GO databases were downloaded from http://geneontology.org/. Fold Enrichment was the ratio of the number of genes observed in our gene list to the number of gene expected in the reference list. The *P*-values were the probability that the number of genes observed in the category occurred by chance (randomly), as determined by the reference list. The complete ChIP-Seq data set is available from GEO (GSE121658).

Statistical analysis

All values are presented as mean ± SEM unless otherwise stated. The two-tailed Student's t-test was used for individual pairwise comparisons. All the data were checked for normal distribution. If the data were not normally distributed, we used Welch's t test. The Tukey-Kramer HSD (honestly significant difference) test was used for multiple pairwise comparisons. The Dunnett test was used for each groups of multiple pairwise versus control. The log-rank test was for statistical analysis of Kaplan-Meier survival curves. P values < 0.05 were considered significant. All statistical analysis were performed with either Graph-Pad Prism (version 6.0, GraphPad, San Diego, CA) or JMP Pro (version 13.0, SAS, Cary, NC).

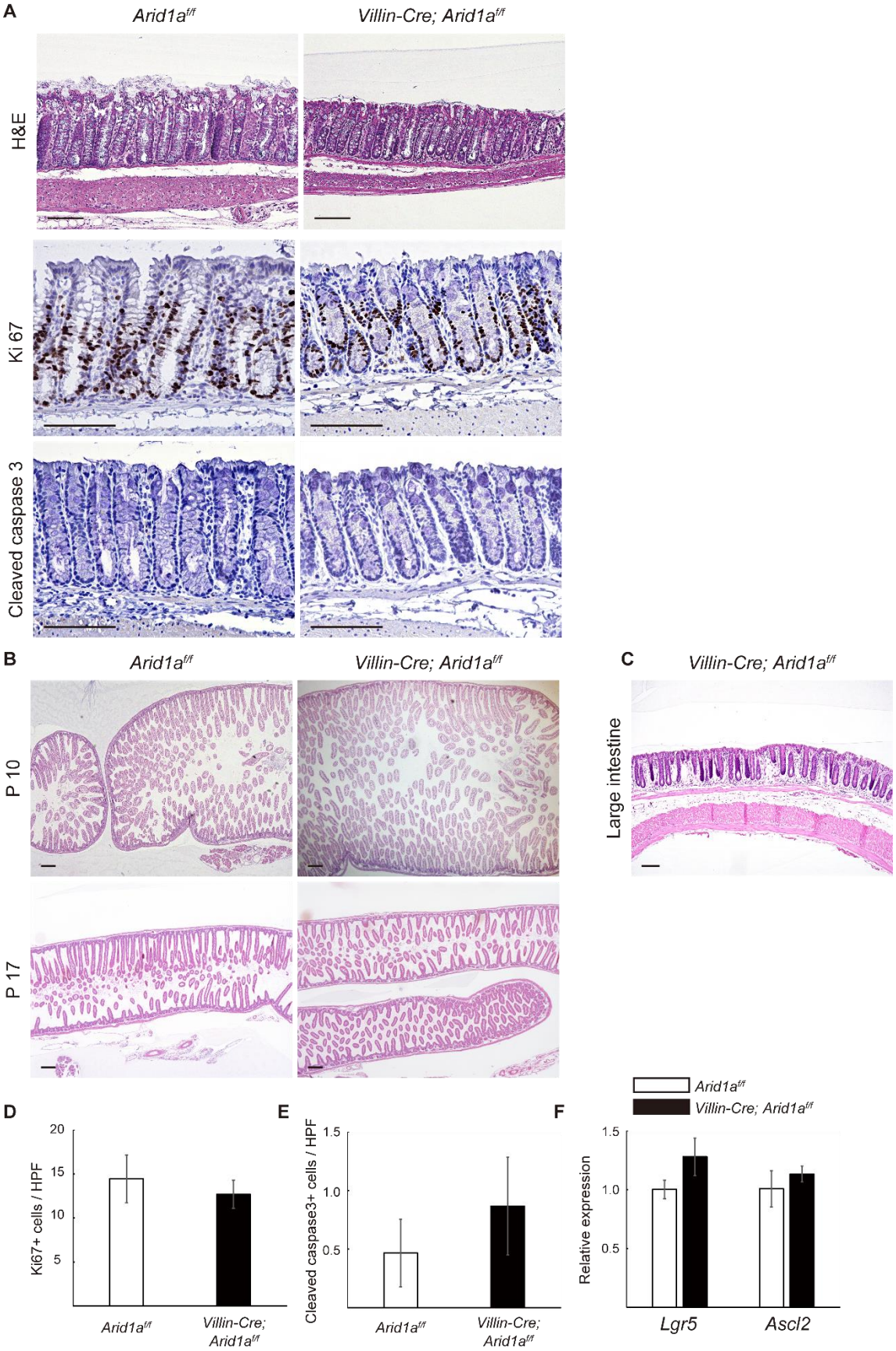
A
Arid1a f/f
Villin-Cre; Arid1a f/f
H&E
Ki 67
Cleaved caspase 3
B
Arid1a f/f
Villin-Cre; Arid1a f/f
P 10
P 17
C
Villin-Cre; Arid1a f/f
Large intestine
D
Ki67+ cells / HPF
20
15
10
5
Arid1a f/f
Villin-Cre; Arid1a f/f
E
Cleaved caspase3+ cells / HPF
1.5
1.0
0.5
Arid1a f/f
Villin-Cre; Arid1a f/f
F
Arid1a f/f
Villin-Cre; Arid1a f/f
Relative expression
1.5
1.0
0.5
Lgr5
Ascl2

Fig. S1. Intestinal *Arid1a*-deletion causes no differences in the large intestines of mice
(*A*) From the top: H&E, Ki67, and cleaved caspase 3 staining of the large intestine in control (left panel) and *Villin-Cre; Arid1a*$^{f/f}$ mice (right panel) at 9 weeks of age. (*B*) H&E staining of the small intestine in control (left panel) and *Villin-Cre; Arid1a*$^{f/f}$ mice (right panel) at the indicated time points. (*C*) H&E staining of the large intestine in *Villin-Cre; Arid1a*$^{f/f}$ mice at 65 weeks of age. (*D*) The number of Ki67 positive cells in the large intestine of control and *Villin-Cre; Arid1a*$^{f/f}$ mice at 9 weeks of age (n = 3). (*E*) The number of cleaved caspase 3 positive cells in the large intestine of control and *Villin-Cre; Arid1a*$^{f/f}$ mice at 9 weeks of age (n = 3). (*F*) Relative expression level of ISC markers in control and *Villin-Cre; Arid1a*$^{f/f}$ mice, as determined by q-PCR using crypt RNA at 9 weeks of age (n=3). Scale bars: 100 μm (*A*, *C*), 200 μm (*B*).Quantitative data are presented as means ± S.D.

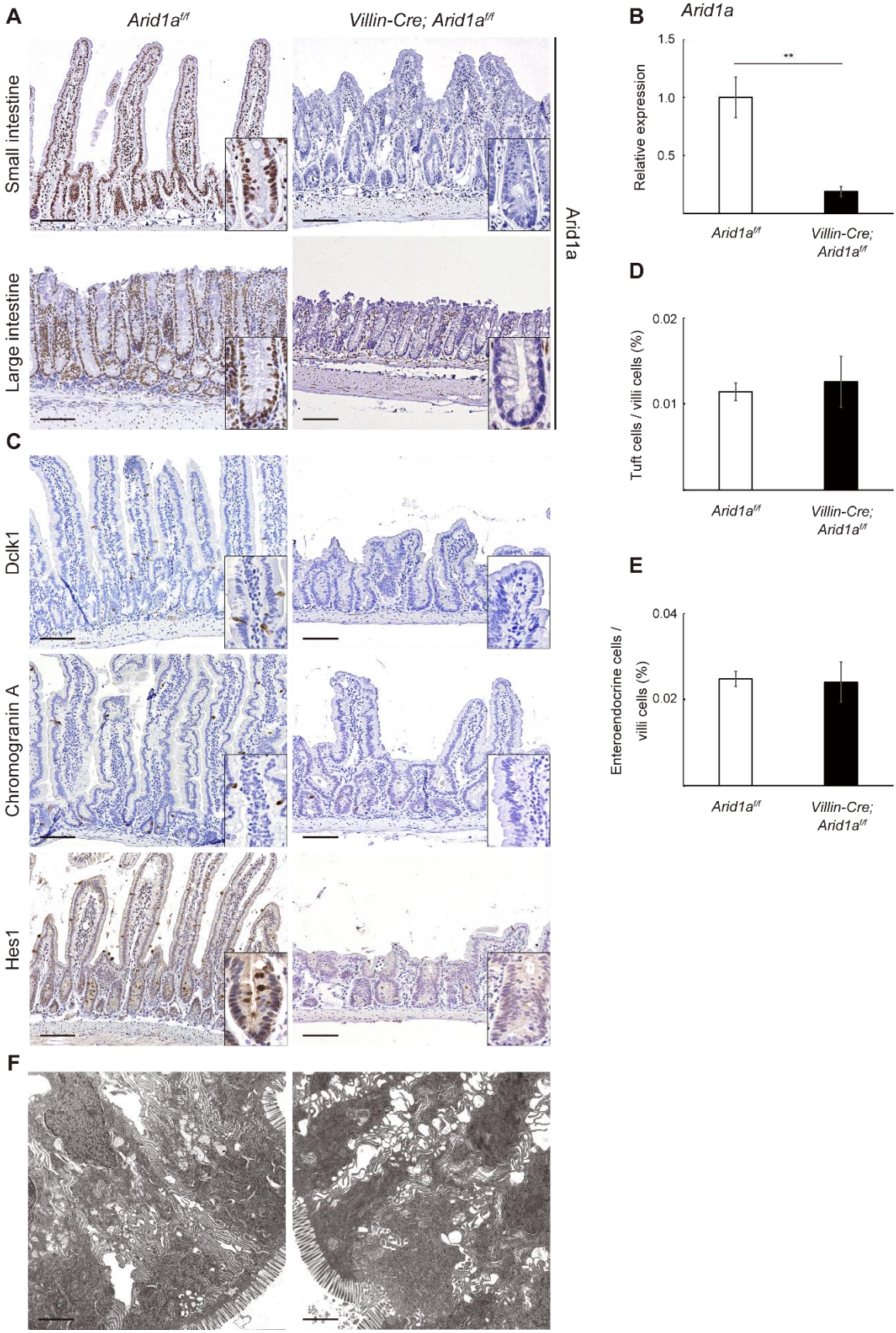
A
Arid1a^f/f
Villin-Cre; Arid1a^f/f
Small intestine
Large intestine
Arid1a
B
Arid1a
Relative expression
1.5
1.0
0.5
**
Arid1a^f/f
Villin-Cre; Arid1a^f/f
C
Dclk1
Chromogranin A
Hes1
D
Tuft cells / villi cells (%)
0.02
0.01
Arid1a^f/f
Villin-Cre; Arid1a^f/f
E
Enteroendocrine cells / villi cells (%)
0.04
0.02
Arid1a^f/f
Villin-Cre; Arid1a^f/f
F

Fig. S2. Intestinal *Arid1a*-deletion causes no differences in the number of tuft and enteroendocrine cells

(*A*) Arid1a staining of the small intestine (top) and large intestine (bottom) in control (left panel) and *Villin-Cre; Arid1a*$^{f/f}$ mice (right panel) at 8 to 9 weeks of age. (*B*) Relative expression level of *Arid1*a in control (n = 3) and *Villin-Cre; Arid1a*$^{f/f}$ mice (n = 5), as determined by q-PCR using crypt RNA at 8 weeks of age. (*C*) From the top: Dclk1, chromogranin A, and Hes1 staining of the small intestines in control (left panel) and *Villin-Cre; Arid1a*$^{f/f}$ mice (right panel) at 8 to 10 weeks of age. (*D-E*) Ratio of the number of tuft (*D*) and enteroendocrine cells (*E*) to all villus cells in control and *Villin-Cre; Arid1a*$^{f/f}$ mice at 8 to 10 weeks of age (n = 3). (*F*) Electron microscopic images of the intestines from control (left panel) and *Villin-Cre; Arid1a*$^{f/f}$ mice (right panel). Scale bars: 100 μm (*A*, *C*), 2 μm (*F*). Quantitative data are presented as means ± S.D. ** $P < 0.01$.

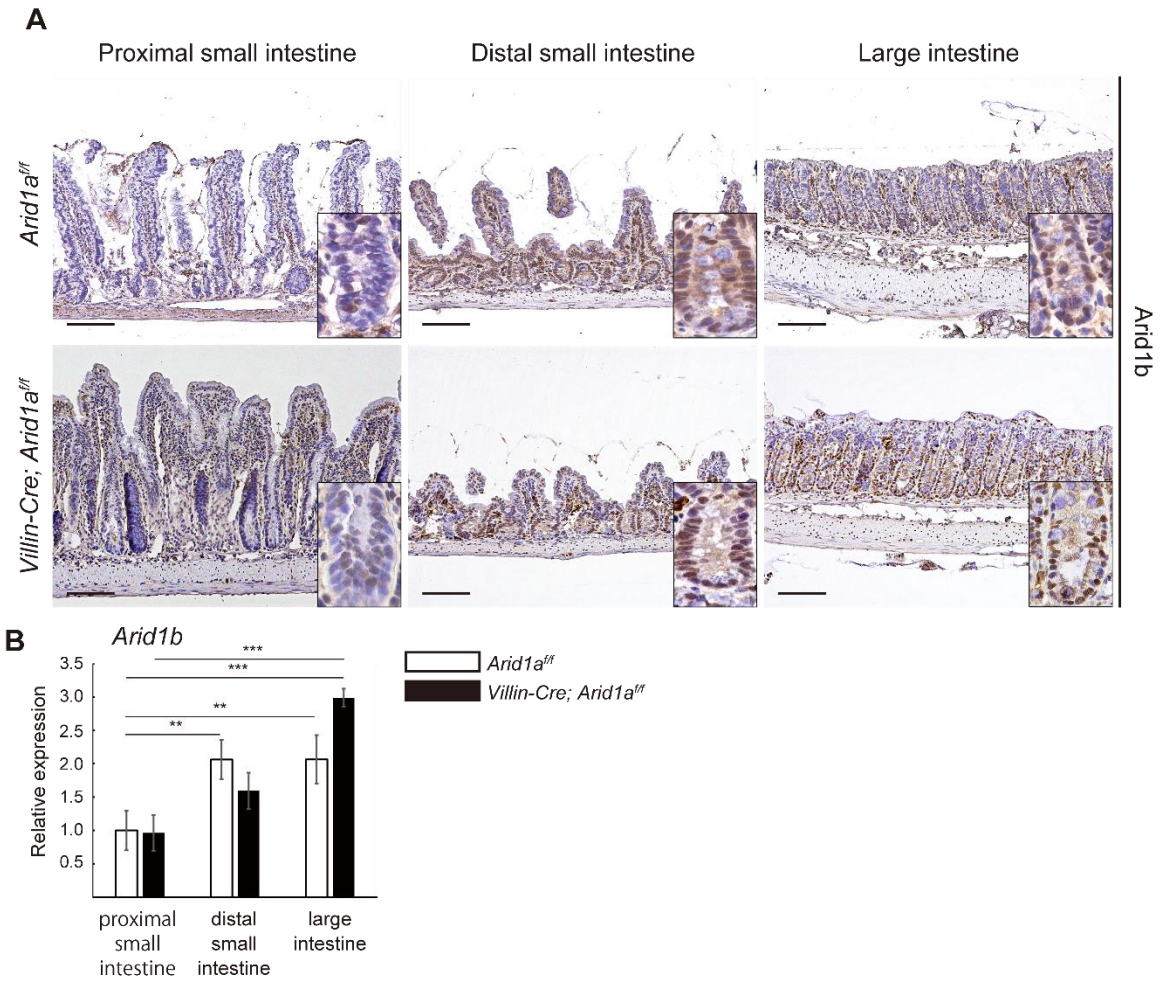

Fig. S3. Arid1b expression is higher in the distal small intestine and large intestine compared to the proximal small intestine

(*A*) Arid1b staining of the proximal (left panel) and distal small intestine (middle panel) and the large intestine (right) in control *Arid1a*$^{f/f}$ (top) and *Villin-Cre; Arid1a*$^{f/f}$ mice (bottom panel) at 9 weeks of age. Scale bars: 100 µm. (*B*) Relative expression level of *Arid1*b in the proximal and distal small intestine and the large intestine of control *Arid1a*$^{f/f}$ and *Villin-Cre; Arid1a*$^{f/f}$ mice, as determined by q-PCR using whole tissue RNA at 9 weeks of age (n = 3). Quantitative data are presented as means ± S.D. ** $P < 0.01$, *** $P < 0.001$.

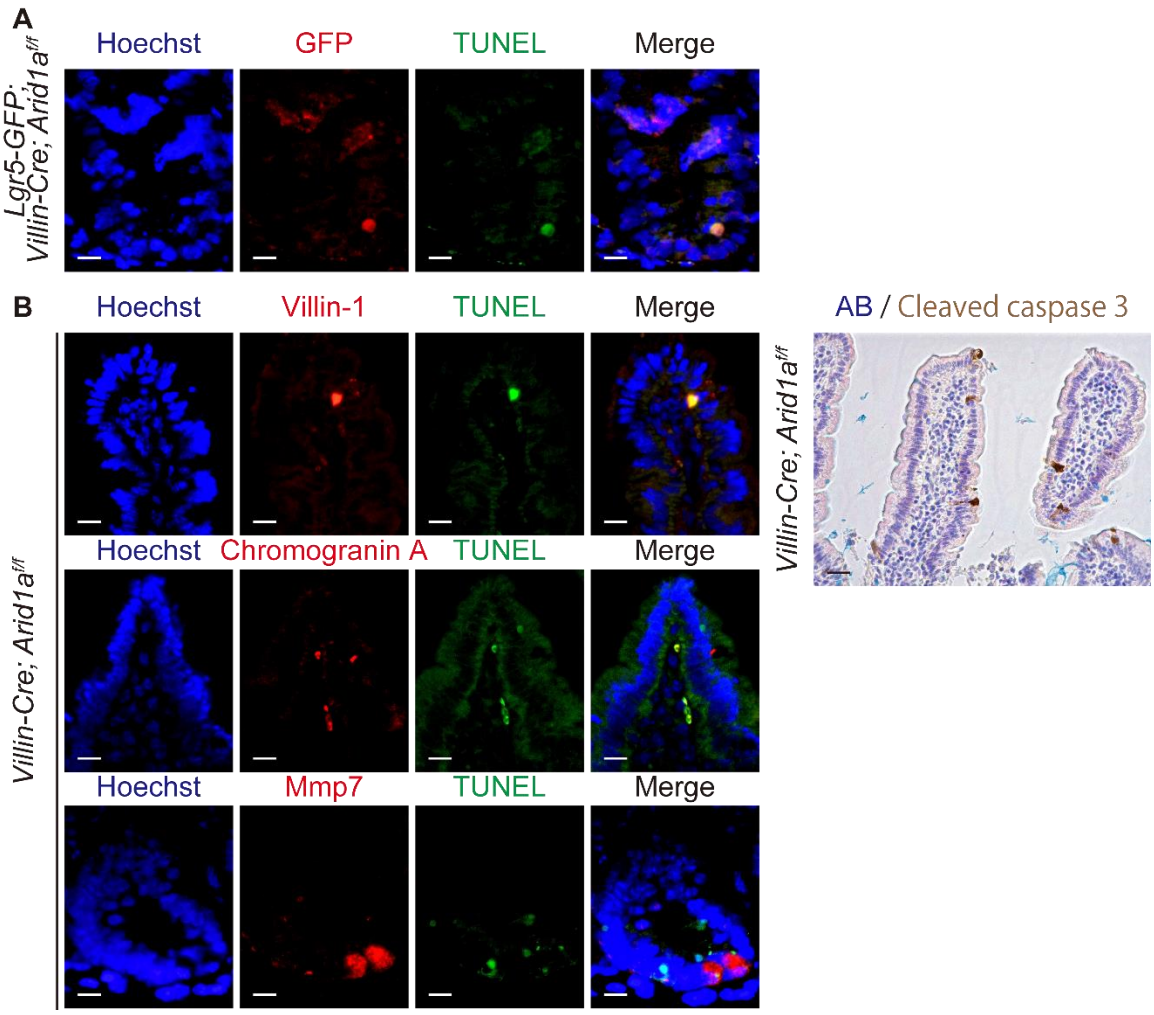

Fig. S4. Apoptosis occurs in both Lgr5^{+} ISCs in crypts and enterocytes in the villi of *Villin-Cre; Arid1a$^{f/f}$* mice

(*A*) Co-staining for GFP/TUNEL/Hoechst in *Lgr5-GFP; Villin-Cre; Arid1a$^{f/f}$* mice at 8 weeks of age. (*B*) Co-staining for Villin-1/TUNEL/Hoechst, chromogranin A/TUNEL/Hoechst, Mmp7/TUNEL/Hoechst, and alcian blue (AB)/cleaved caspase 3 in *Villin-Cre; Arid1a$^{f/f}$* mice at 8 weeks of age. Scale bars: 100 μm (*A*, *B*).

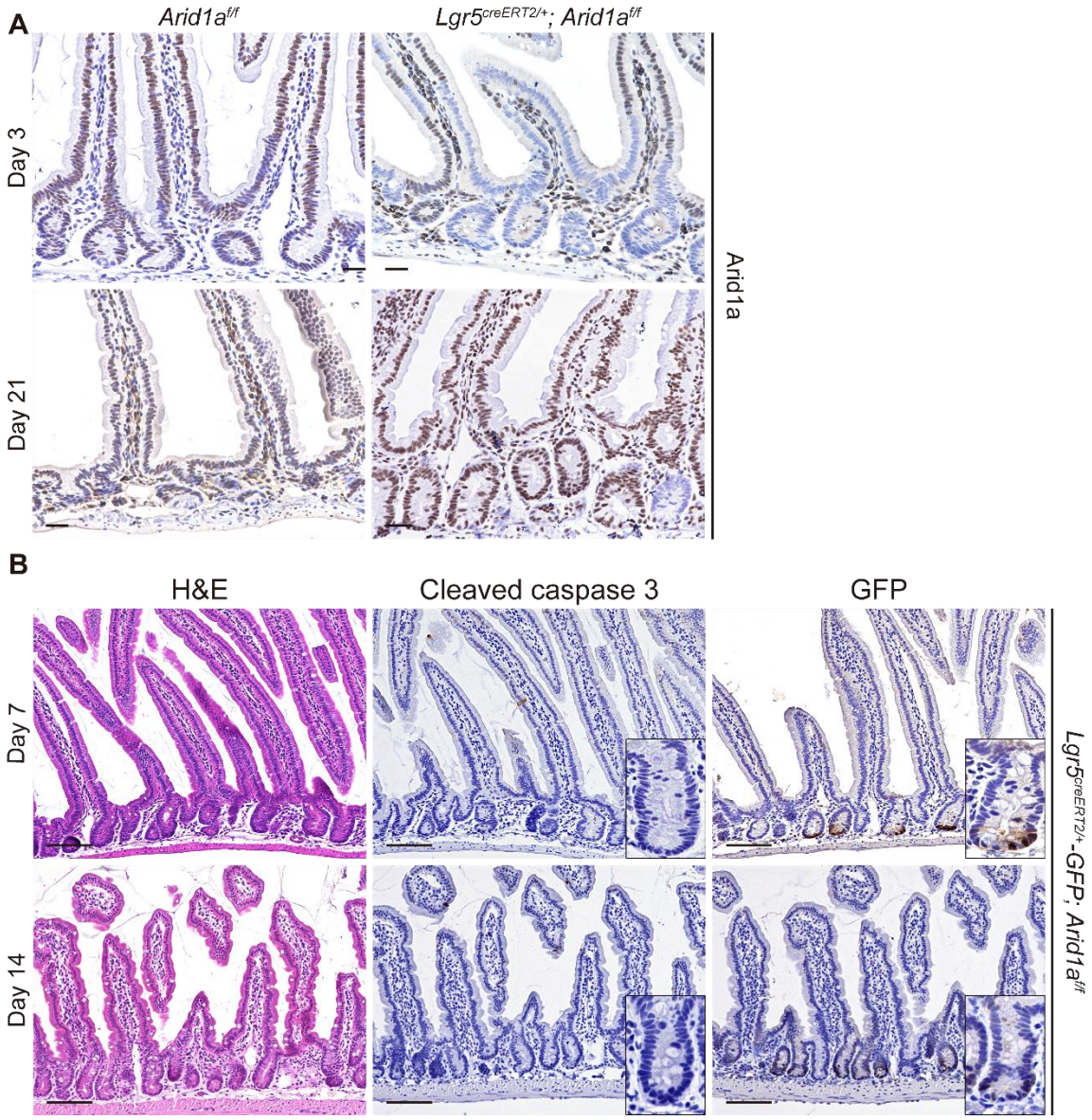

Fig. S5. Intestinal *Arid1a*-deletion in Lgr5^{+} ISCs does not perturb homeostasis in the small intestine at 1 and 2 weeks after *Arid1a*-deletion in Lgr5^{+} ISCs

(*A*) Arid1a staining of control *Arid1a*$^{f/f}$ (left panel) and *Lgr5*$^{CreERT2/+}$*; Arid1a*$^{f/f}$ mice (right panel) at 3 and 21 days after the last tamoxifen injection. (*B*) IHC analysis for H&E, cleaved caspase 3, and GFP in *Lgr5*$^{CreERT2/+}$*-GFP; Arid1a*$^{f/f}$ intestines at 1 and 2 weeks after the last tamoxifen injection. Scale bars: 50 μm (*A*), 100 μm (*B*).

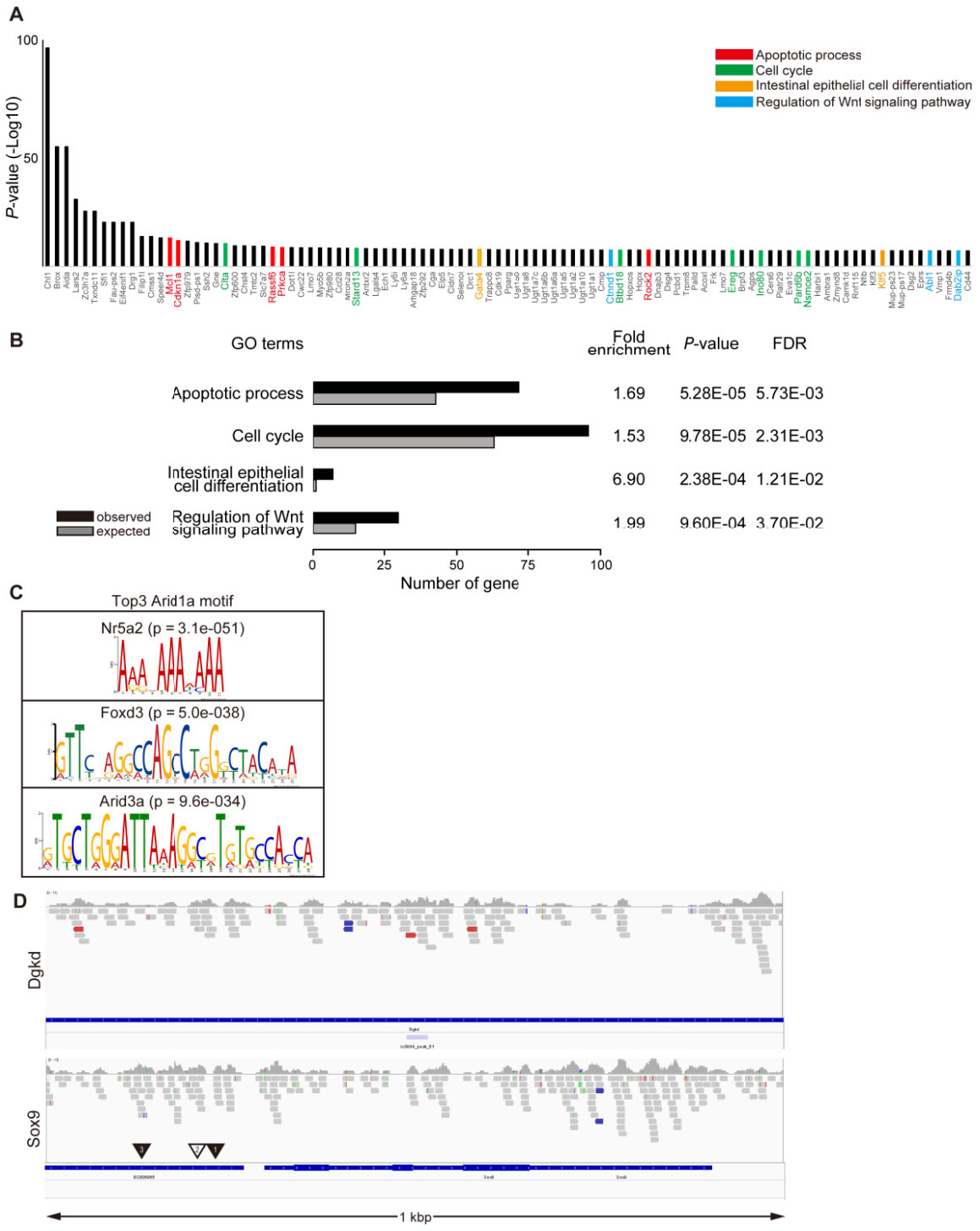

Fig. S6. Arid1a regulates various gene expression

(*A*) Depicted are the top100 gene targets in the intestine with minimum *P*-values identified by ChIP-Seq peak calling analysis. (*B*) Summary of results from Gene Ontology analysis. (*C*) The binding sites are associated with DNA sequence-specific motifs that overlap with Nr5a2, Foxd3, and Arid3a motifs. (*D*) Sequencing coverage histograms that aligned to *Dgkd* (top) and *Sox9* (bottom). The black triangles indicate the DNA binding sites (site 1 and site 3) as confirmed by ChIP assay. The white triangle indicates the additional DNA binding site (site 2). Red line: The insert size of paired

reads is greater than 1000 bp. Blue line: The insert size of paired reads is smaller than 50 bp. Green line: The orientation of paired reads is anomalous.

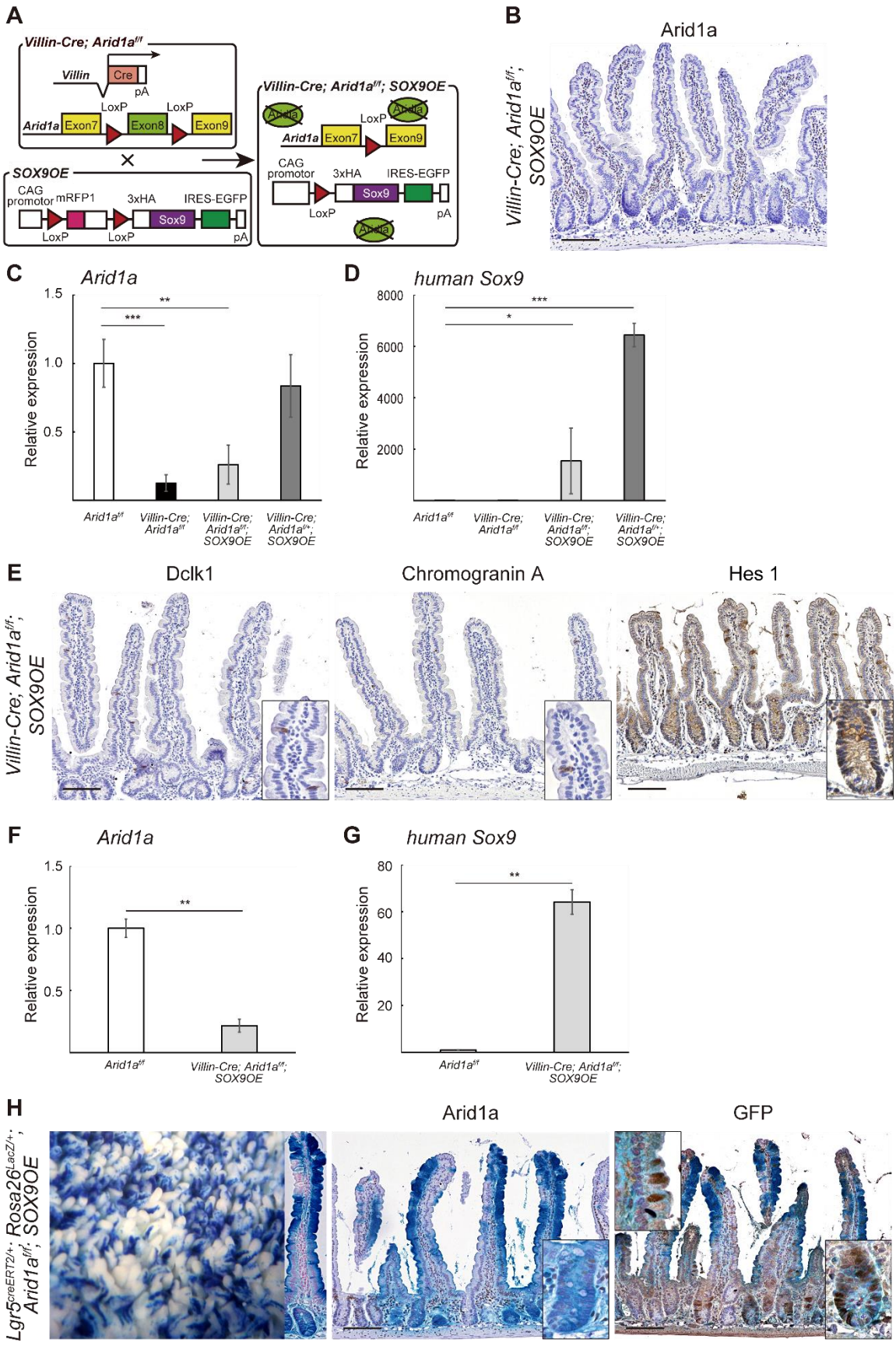
A
Villin-Cre; Arid1a f/f
Villin
Cre
pA
LoxP
LoxP
Arid1a
Exon7
Exon8
Exon9
SOX9OE
CAG promotor
mRFP1
3xHA
IRES-EGFP
Sox9
LoxP
LoxP
pA
Villin-Cre; Arid1a f/f; SOX9OE
Arid1a
LoxP
Arid1a
Arid1a
Exon7
Exon9
CAG promotor
3xHA
IRES-EGFP
Sox9
LoxP
pA
Arid1a
B
Arid1a
Villin-Cre; Arid1a f/f; SOX9OE
C
Arid1a
Relative expression
1.5
1.0
0.5
**
***
Arid1a f/f
Villin-Cre; Arid1a f/f
Villin-Cre; Arid1a f/+; SOX9OE
Villin-Cre; Arid1a f/f; SOX9OE
D
human Sox9
Relative expression
8000
6000
4000
2000
***
*
Arid1a f/f
Villin-Cre; Arid1a f/f
Villin-Cre; Arid1a f/+; SOX9OE
Villin-Cre; Arid1a f/f; SOX9OE
E
Dclk1
Chromogranin A
Hes 1
Villin-Cre; Arid1a f/+; SOX9OE
F
Arid1a
Relative expression
1.5
1.0
0.5
**
Arid1a f/f
Villin-Cre; Arid1a f/f; SOX9OE
G
human Sox9
Relative expression
80
60
40
20
**
Arid1a f/f
Villin-Cre; Arid1a f/f; SOX9OE
H
Arid1a
GFP
Lgr5 creERT2/+; Rosa26 LacZ/+; Arid1a f/f; SOX9OE

Fig. S7. Expression of *Arid1a* and *Sox9* in *Villin-Cre; Arid1a$^{f/f}$; SOX9OE* intestines, spheroids generated from *Villin-Cre; Arid1a$^{f/f}$; SOX9OE* intestines, and in *Lgr5$^{CreERT2/+}$; Rosa$^{lacZ/+}$; Arid1a$^{f/f}$; SOX9OE* mice

(*A*) Schema of recombination in *Villin-Cre; Arid1a$^{f/f}$; SOX9OE* mice. (*B*) Staining for Arid1a in *Villin-Cre; Arid1a$^{f/f}$; SOX9OE* mice at 8 weeks of age. (*C-D*) Relative expression levels of *Arid1a* (*C*) and *human Sox9* (*D*) in control *Arid1a$^{f/f}$* (n = 3), *Villin-Cre; Arid1a$^{f/f}$* (n = 5), *Villin-Cre; Arid1a$^{f/f}$; SOX9OE* (n = 3), and *Villin-Cre; Arid1a$^{f/+}$; SOX9OE* (n = 3) intestines, as determined by q-PCR using crypt RNA at 8 weeks of age. (*E*) Staining for Dclk1 (left panel), chromogranin A (middle panel), and Hes1 (right panel) in *Villin-Cre; Arid1a$^{f/f}$; SOX9OE* mice at 8 weeks of age. (*F-G*) Relative expression levels of *Arid1a* (*F*) and *human Sox9* (*G*) in spheroids cultured from crypts of control *Arid1a$^{f/f}$* and *Villin-Cre; Arid1a$^{f/f}$; SOX9OE* intestines, as determined by q-PCR using spheroid RNA (n = 3). (*H*) Macroscopic image of LacZ staining (left panel), staining for Arid1a and LacZ (middle panel), and staining for GFP and LacZ (right panel) in *Lgr5$^{CreERT2/+}$; Rosa$^{lacZ/+}$; Arid1a$^{f/f}$; SOX9OE* mice at 3 days after the last tamoxifen injection. Scale bars: 100 μm (*B, E, H*). Quantitative data are presented as means ± S.D. * $P < 0.05$, ** $P < 0.01$, *** $P < 0.001$.

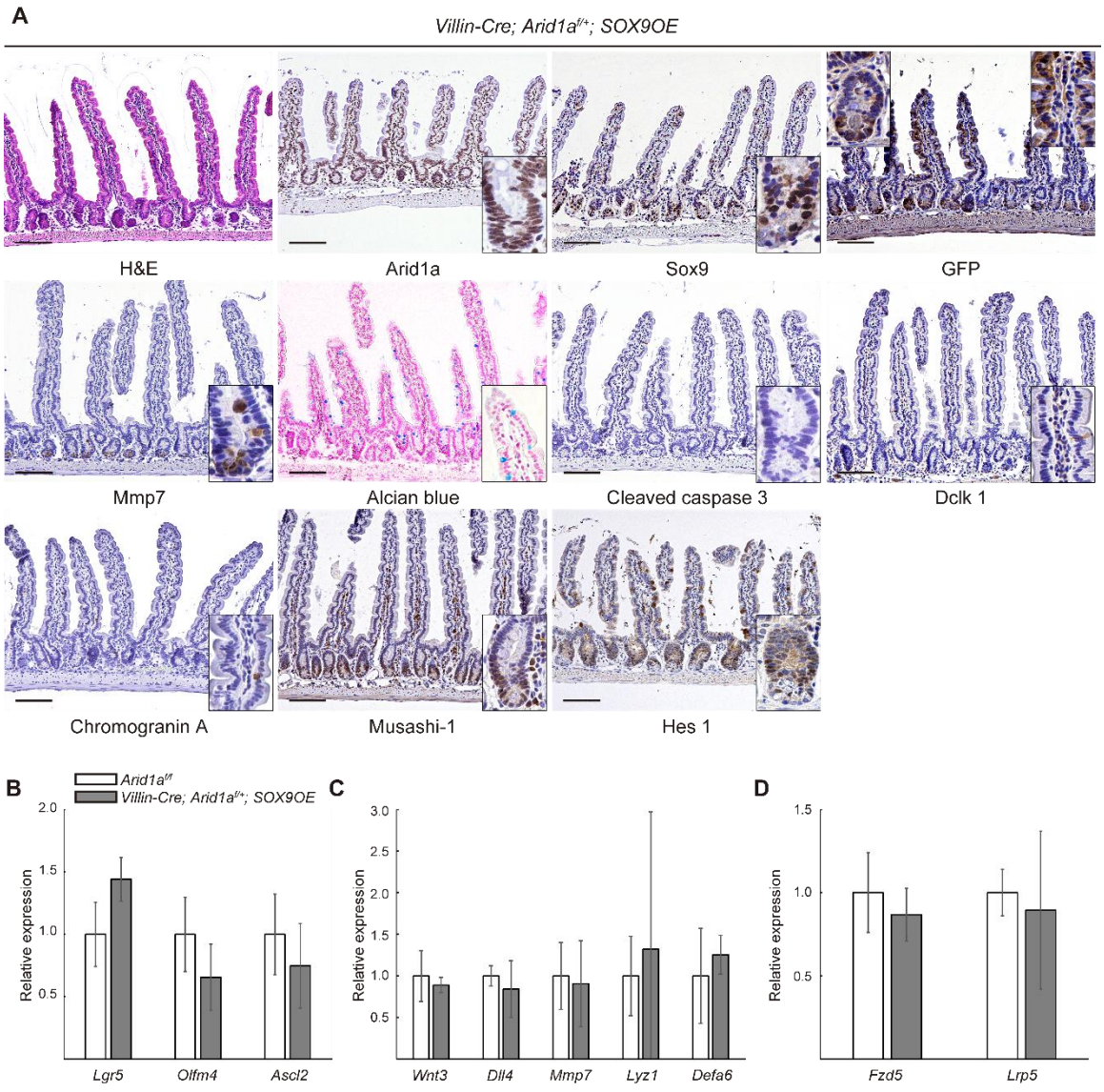

Fig. S8. There are no differences between *Villin-Cre; Arid1a$^{f/+}$; SOX9OE* and control *Arid1a$^{f/f}$* mice in intestinal architecture, cellular differentiation, and relative expression levels of ISC markers and Wnt receptor genes

(*A*) H&E, Arid1a, Sox9, GFP, Mmp7, alcian blue, cleaved caspase 3, Dclk1, chromogranin A, Musashi-1, and Hes1 staining of the small intestines in *Villin-Cre; Arid1a$^{f/+}$; SOX9OE* mice at 8 weeks of age. Scale bars: 100 μm. (*B-D*) Relative expression levels of ISC markers (*B*), Paneth cell markers (*C*), and Wnt receptor genes (*D*) in control *Arid1a$^{f/f}$* and *Villin-Cre; Arid1a$^{f/+}$; SOX9OE* intestines, as determined by q-PCR using crypt RNA (n = 3). Quantitative data are presented as means ± S.D.

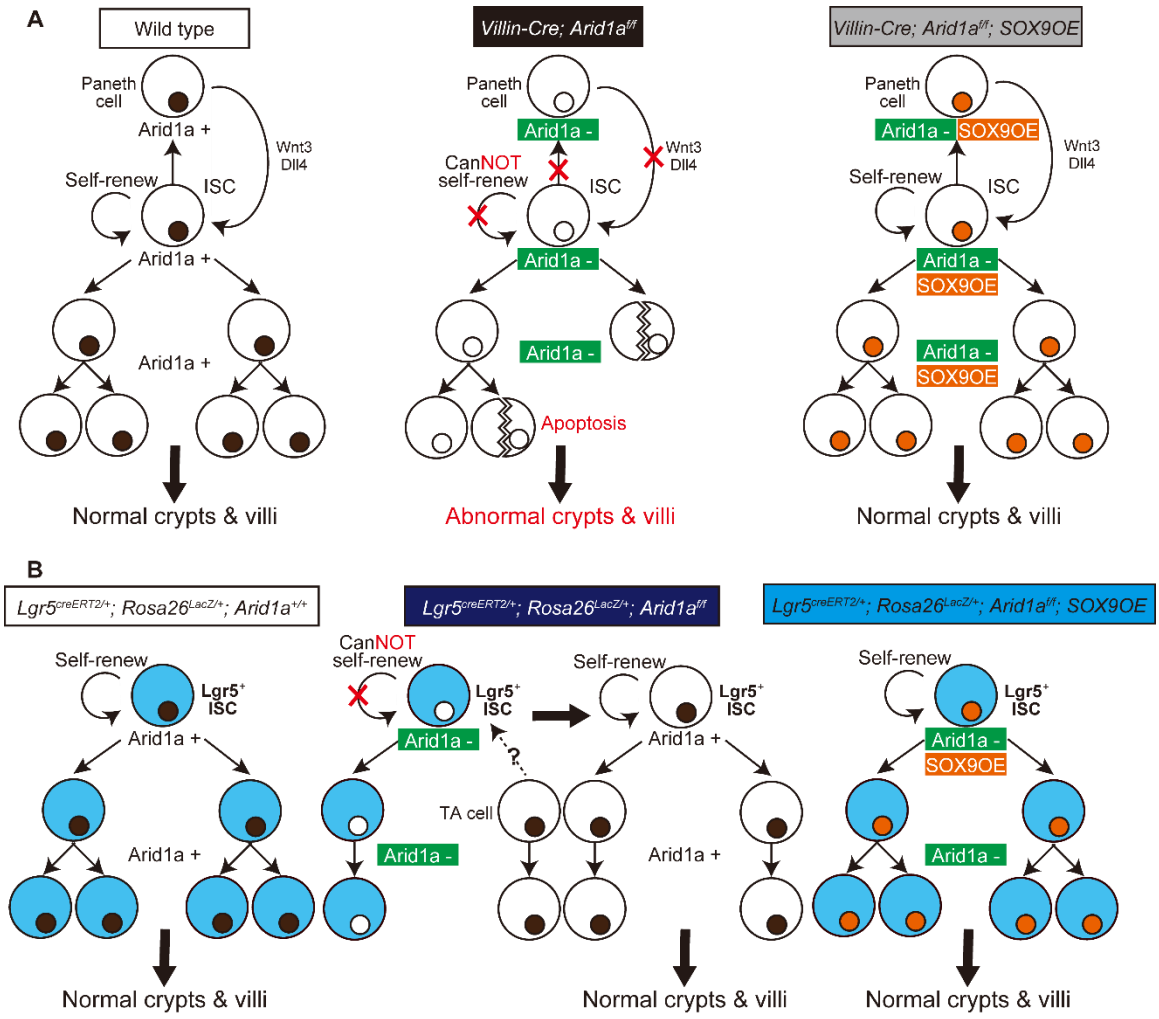

Fig. S9. Arid1a is indispensable for maintenance of ISCs and intestinal homeostasis in the small intestines of mice

(*A*) Schema of *Arid1a*-deletion in intestinal epithelial cells. Deletion of *Arid1a* in intestinal epithelial cells results in impaired self-renewal of ISCs, depletion of Paneth cells, which produce Wnt3 and Dll4, increased apoptosis in cells of crypts and villi, and abnormal crypt-villous architecture in *Villin-Cre; Arid1a*$^{f/f}$ mice (middle panel). Deletion of *Arid1a* concomitant with *Sox9* overexpression in intestinal epithelial cells restores ISCs and Paneth cells as well as the normal architecture of crypts and villi, and prevents apoptosis in *Villin-Cre; Arid1a*$^{f/f}$*; SOX9OE* mice (right panel). (*B*) Schema of *Arid1a*-deletion in Lgr5^{+} ISCs with lineage tracing. Deletion of *Arid1a* in Lgr5^{+} ISCs results in impaired self-renewal of ISCs. However, the intestinal architecture of crypts and villi is normal in *Lgr5*$^{CreERT2/+}$*; Rosa*$^{lacZ/+}$*; Arid1a*$^{f/f}$ mice, in which *Arid1a*-deleted Lgr5^{+} ISCs are compensated and replaced by Arid1a+ Lgr5^{+} ISCs, and ISCs and their progeny cells are negative for lacZ staining (middle panel). Deletion of *Arid1a* concomitant with *Sox9* overexpression in Lgr5^{+} ISCs restores self-renewal of *Arid1a*-deleted Lgr5^{+} ISCs, and thereby, ISCs and their progeny cells are positive for lacZ staining in *Lgr5*$^{CreERT2/+}$*; Rosa*$^{lacZ/+}$*; Arid1a*$^{f/f}$*; SOX9OE* mice (right panel).

Table S1. A list of genes included in each GO terms

GO terms	Gene									
Apoptotic process	Cflar	Gpx1	Rbm25	Traf1	Pak1	Bcl2l14	Arl6ip5	Irf1	Nek6	Fhit
	Prkca	Ube2d3	Blcap	Map3k5	Nupr1	Itgav	Acaa2	Shf	Cdkn1a	Lgals7
	Ep300	Fam3b	Gsn	Rnf186	Naip2	Trim69	Dab2ip	Epha2	Fgfr2	Naip1
	Krt8	Cdip1	Etv6	Rassf6	Rb1	Gadd45b	Gsk3b	Rock2	Stk25	Egln3
	Bcl2l1	Tnfsf12	Dedd	Sap30bp	Babam2	Ero1l	Phlpp1	Nfatc4	Smad3	Abl1
	Mecom	Gabarap	Psen1	Tax1bp1	Sgms1	Mef2d	Naif1	Pls1	Casp8	Purb
	Rffl	Dyrk2	Mtch2	Naip5	Sort1	Ddit4	Shb	Rmdn3	Mcl1	Vil1
	Cdca7	Birc6								
Cell cycle	Fbxl18	Mapk6	Rhoa	Camk2d	Btbd18	Hnrnpu	Rab11a	Specc1l	Irf1	Tlk1
	Bcl2l1	Pard6b	Pibf1	Ereg	Exd1	Babam2	Wee1	Smpd3	Blcap	Usp3
	Gadd45a	Phb2	Cdkn1a	Clta	Nsmce2	Ect2	Cdk6	Ezh2	Ep300	Zfyve19
	Tubgcp4	Nsun2	Lin9	Mei1	Epb41l2	Cdk11b	Incenp	Dab2ip	Ctnnb1	Terb2
	Csnk1a1	Txnip	Rb1	Rad51	Wapl	Ezr	Gsk3b	Rock2	Nup153	Uba3
	Fbxw11	Knstrn	Mtus1	Anapc2	Cdkn1b	Msh5	Tcf7l2	Tubg2	Mad2l1bp	Acvr1
	Nek6	Stard13	Cep192	Cep55	Ckap5	Cltc	Pds5a	Aurkb	Gnai3	Ptpn6
	Kif3b	Cdc25b	Cables2	Appl1	Insc	Cd2ap	Syne2	Smad3	Ppp2ca	Camk2d
	Ino80	Chtf8	Birc6	Usp37	Rcc1	Rabgap1	Phf23	Src	Sptbn1	Hjurp
	Mybl2	Myh9	Eps8	Evi5	Chmp2b	Notch2				
Intestinal epithelial cell differentiation	Gata4	Cbfa2t2	Gata6	Cdh1	Klf5	Cdx2	C1galt1			
Regulation of Wnt signaling pathway	Rnf43	Ctdnep1	Fermt1	Snx3	Lrp4	Cdh3	Trpm4	Smarca4	Nrarp	Psen1
	Abl1	Cdh1	Csnk1a1	Ctnnd1	Mbd2	Sulf2	Gsk3b	Tmem237	Src	Lgr4
	Znrf3	Dab2ip	Fgfr2	Nfatc4	Smad3	Axin2	Tcf7l2	Lrp6	Notum	Rbms3

Table S2. A list of used primers in RT-PCR and ChIP-PCR experiments

Gene	primer	sequence	Gene	primer	sequence
Gapdh	forward	AGGTCGGTGTGAACGGATTTG	*Fzd5*	forward	GGTGTGCCAGGAAATCACG-
	reverse	TGTAGACCATGTAGTTGAGGTCA		reverse	CACAAGCGGCCAGAATTGG-
Mmp7	forward	CTTACCTCGGATCGTAGTGGA	*Lrp5*	forward	AAGGGTGCTGTGTACTGGAC-
	reverse	CCCCAACTAACCCTCTTGAAGT		reverse	AGAAGAGAACCTTACGGGACG-
Lyz1	forward	GGAATGGATGGCTACCGTGG	*Lrp6*	forward	TTGTTGCTTTATGCAAACAGACG-
	reverse	CATGCCACCCATGCTCGAAT		reverse	GTTCGTTTAATGGCTTCTTCGC-
Defa6	forward	CCTTCCAGGTCCAGGCTGAT	*Dll4*	forward	TTCCAGGCAACCTTCTCCGA-
	reverse	TGAGAAGTGGTCATCAGGCAC		reverse	ACTGCCGCTATTCTTGTCCC-
Lgr5	forward	TCCTAGAAGAGTTACGTCTTGCT	*Wnt2b*	forward	CACCCGGACTGATCTTGTCT-
	reverse	CCTTGGGAATGTGTGTCAAAGC		reverse	TGTTTCTGCACTCCTTGCAC-
Olfm4	forward	CAGCCACTTTCCAATTTCACTG	*Wnt4*	forward	AACGGAACCTTGAGGTGATG-
	reverse	GCTGGACATACTCCTTCACCTTA		reverse	GGACGTCCACAAAGGACTGT-
Ascl2	forward	AAGCACACCTTGACTGGTACG-	*Wnt5a*	forward	CACGCTATACCAACTCCTCTGC-
	reverse	AAGTGGACGTTTGCACCTTCA-		reverse	AATATTCCAATGGGCTTCTTCATGGC-
Sox9	forward	AACATGGAGGACGATTGGAG-	*Wnt6*	forward	CGGAGACGATGTGGACTT-
	reverse	TCCCCTCAAAATGGTAATGAG-		reverse	GGAACCCGAAAGCCCATG-
Axin2	forward	TGACTCTCCTTCCAGATCCCA-	*Arid1a*	forward	GACCCCTCAGTCATCCAGTC-
	reverse	TGCCCACACTAGGCTGACA-		reverse	GAGTATGGGTTAGTCCCACCA-
Tcf4	forward	CGAAAAGTTCCTCCGGGTTTG-	*Arid1b*	forward	GTTGTATGGGATGGGTACTCACC-
	reverse	CGTAGCCGGGCTGATTCAT-		reverse	CTGGTTGTAGTATGGCTGCTG-
Hes1	forward	CGGCATTCCAAGCTAGAGAAGG-	*hu Sox9*	forward	AGCGAACGCACATCAAGAC-
	reverse	GGTAGGTCATGGCGTTGATCTG-		reverse	CTGTAGGCGATCTGTTGGGG-
Wnt3	forward	TGGAACTGTACCACCATAGATGAC-	*Sox9 site1*	forward	ACACCAGCTTCGTTGAACCAGAG-
	reverse	ACACCAGCCGAGGCGATG-		reverse	GGAAGCAAATGTTTGGGTGACTCA-
Wnt6	forward	CGGAGACGATGTGGACTT-	*Sox9 site2*	forward	ACTTGTCAGTTCAAGGTCGGCGTG-
	reverse	GGAACCCGAAAGCCCATG-		reverse	TGTGGTGACTGGAGCTTCTGCTG-
Fzd4	forward	TGCCAGAACCTCGGCTACA-	*Sox9 site3*	forward	CGAGCTTTTCAAAAGCATCCCAAAGA-
	reverse	ATGAGCGGCGTGAAAGTTGT-		reverse	TGATAAAGCGAATCGGCCTGTATC-

References

1. Sato T, *et al.* (2011) Paneth cells constitute the niche for Lgr5 stem cells in intestinal crypts. *Nature* 469(7330):415-418.
2. Barker N, *et al.* (2007) Identification of stem cells in small intestine and colon by marker gene Lgr5. *Nature* 449(7165):1003-1007.
3. Sato T, *et al.* (2009) Single Lgr5 stem cells build crypt-villus structures in vitro without a mesenchymal niche. *Nature* 459(7244):262-265.
4. Sato T & Clevers H (2013) Growing self-organizing mini-guts from a single intestinal stem cell: mechanism and applications. *Science* 340(6137):1190-1194.
5. Subramanian A, *et al.* (2005) Gene set enrichment analysis: a knowledge-based approach for interpreting genome-wide expression profiles. *Proc Natl Acad Sci U S A* 102(43):15545-15550.
6. Miyoshi H & Stappenbeck TS (2013) In vitro expansion and genetic modification of gastrointestinal stem cells in spheroid culture. *Nat Protoc* 8(12):2471-2482.